PRAMANA — journal of physics

Vol. 78, No. 2
February 2012
pp. 277–288

A comparative study of the ionic keV X-ray line emission from plasma produced by the femtosecond, picosecond and nanosecond duration laser pulses

V ARORA*, P A NAIK, B S RAO and P D GUPTA

Laser Plasma Division, Raja Ramanna Centre for Advanced Technology, Indore 452 013, India
*Corresponding author. E-mail: arora@rrcat.gov.in

MS received 29 March 2011; revised 4 July 2011; accepted 15 July 2011

Abstract. We report here an experimental study of the ionic keV X-ray line emission from magnesium plasma produced by laser pulses of three widely different pulse durations (FWHM) of 45 fs, 25 ps and 3 ns, at a constant laser fluence of $\sim 1.5 \times 10^4$ J cm^{-2}. It is observed that the X-ray yield of the resonance lines from the higher ionization states such as H- and He-like ions decreases on decreasing the laser pulse duration, even though the peak laser intensities of 3.5×10^{17} W cm^{-2} for the 45 fs pulses and 6.2×10^{14} W cm^{-2} for the 25 ps pulses are much higher than 5×10^{12} W cm^{-2} for the 3 ns laser pulse. The results were explained in terms of the ionization equilibrium time for different ionization states in the heated plasma. The study can be useful to make optimum choice of the laser pulse duration to produce short pulse intense X-ray line emission from the plasma and to get the knowledge of the degree of ionization in the plasma.

Keywords. X-ray spectroscopy; laser-produced plasma; ionization equilibrium.

PACS Nos 52.50.Jm; 52.70.La; 07.85.Nc

1. Introduction

X-ray line radiation emitted from the laser-produced plasmas is broadly classified into inner-shell line emission and ionic line emission [1]. The inner-shell X-ray line radiation is produced by the hot electrons generated during the interaction of the ultrashort, ultraintense laser pulses with the target [2]. The hot electrons penetrate into the cold target material to produce the characteristic X-ray line radiation (K-α, K-β, L-α, etc.). The photon number, the source size and the pulse duration of the K-α emission are determined by the incident electron energy spectrum and the reabsorption of the radiation in the bulk target [2,3]. This line radiation is useful for investigating fast electrons, like their transport into the target [4]. The duration of the characteristic X-ray line radiation is of the order of the laser pulse duration and it originates from the micron-sized source. These features make it suitable for studying the time evolution of ultrafast physical, chemical and biological processes [5], and phase contrast imaging [6]. On the other hand, the ionic line

DOI: 10.1007/s12043-011-0218-9; ***e*Publication: 18 January 2012**

emission is due to the electronic transitions in the highly charged ionic species (H-like, He-like) present in the plasma heated to a high temperature. The spectral and temporal characteristics of such radiation depend on plasma parameters, viz. electron density, temperature, average degree of ionization and opacity of the hot plasma medium [7,8]. The pulse duration of the ionic line radiation can be less than a picosecond [9] and is governed by the heating laser pulse duration, hydrodynamical parameters and ionization dynamics [9–12]. Milchberg *et al* [10] have theoretically outlined the factors controlling the X-ray pulse emission from a solid target heated by an intense femtosecond duration laser. The yield of sub-keV X-ray line radiation was predicted to be lower than that of the recombination radiation due to collisional de-excitation of the excited states at solid density.

The study of the intense keV X-ray line emission from dense and high-temperature plasmas produced by short and ultrashort laser pulses has been a topic of much current interest. For example, the X-ray line emission from H- and He-like ions in the photon energy range of $\sim$1–2 keV in plasmas produced from moderate-Z targets has applications in pumping of the inner shell X-ray lasers [13], backlighting of the fuel pellets in laser-driven inertial confinement fusion [14], time-resolved X-ray diffraction [15] etc. High conversion efficiency of the laser energy into the X-ray line radiation is a prerequisite for the above applications. X-ray line emission is also used to derive diagnostic information on electron temperature, density and ionization states of the plasma, by comparing the measured line shapes and the ratio of the intensities with the calculations [16].

The necessary condition for the K-shell ionic X-ray line emission is the abundance of H- and He-like ions in the plasma. Highly charged ionic species are produced by collisional ionization in a high-temperature plasma or by optical field ionization of matter on irradiation with high intensity laser pulse [17]. The temperature of the plasma depends on laser parameters, viz. intensity, wavelength, pulse duration etc. [1,18]. Intense sub-picosecond ionic X-ray pulses are produced when both the plasma density and the temperature are high [9]. In the short-duration laser pulse-produced plasma, due to negligible expansion and heat conduction during the laser pulse, the above conditions can be realized. However, the ionization dynamics plays an important role in determining the charge state distribution in the short-duration laser-produced plasma [12]. Moreover, X-ray emission region of such a plasma undergoes a change in density and temperature on a time-scale much shorter or comparable to the ionization equilibrium time-scales [19,20]. Short-duration ionic X-ray line radiation can be generated from the plasma produced by ultrashort duration laser pulse while nanosecond lasers give nanosecond or larger X-ray emissions. The ionic line emission from ultrashort laser-produced plasmas is also a possible ultrashort X-ray source for applications in ultrafast dynamics [15]. In such a scenario, the laser pulse duration should be optimum for efficient ultrashort duration X-ray emission, as well as for the generation of highly charged ionic species in the plasma. A study of the ionic X-ray line emission from the plasmas produced by femtosecond, picosecond and nanosecond duration laser pulses can bring out the role of ionization dynamics and hydrodynamic parameters.

Several studies have been reported on the effect of the laser pulse duration [9,21–25] on the X-ray line emission from rapidly evolving plasmas. For instance, time integrated sub-keV (10 Å–70 Å) X-ray emission from the laser-produced carbon plasma as a function of pulse duration (130 fs–1.3 ps) was studied by Altenbernd *et al* [22]. They observed that at a constant laser intensity, the continuum X-ray emission is much larger for the

shorter laser pulse duration, and the H-like lines are much weaker than those from He-like ions. On the other hand, at a constant laser fluence (2.2×10^4 J cm^{-2}), they noted that the spectral shapes and relative fractions of individual lines and continuum are nearly independent of the pulse duration. For instance, in the pulse duration range of their study, the intensity of the X-ray line from H-like ions from plasma produced with the longest laser pulse duration (1.3 ps) is only three times more in comparison to that with the shortest pulse duration (130 fs) produced plasma. In the keV X-ray energy range, the line emission from aluminum plasma has been studied by Limpouch *et al* [24] as a function of laser pulse duration in a range of 1.5 ps–1 ns, for fixed laser fluence [$(5–6) \times 10^6$ J cm^{-2}]. They observed that the conversion efficiency of both H- and He-like resonance lines increased with pulse duration, and this was supported by theoretical modelling of X-ray emission using the standard particle-in-cell code with appropriate modification for shorter laser pulse interaction with matter. They noted that when going from 1.5 ps to 1 ns, the peak intensity of the He-α resonance line increases slightly but the intensity of the H-α line increases by two orders of magnitude. However, in this study, the smallest value of the laser pulse duration was limited to 1.5 ps. It is desirable to have more theoretical and experimental data on the effect of pulse duration on X-ray emission. There is no study on the keV X-ray line emission which compares the relative X-ray yield from the plasmas produced by laser pulses of duration extending from nanosecond to femtosecond at a constant laser fluence.

In this paper, we report a spectroscopic study of the X-ray emission from magnesium plasma produced by laser pulses of femtosecond, picosecond and nanosecond duration, at laser intensities ranging from $\sim 5 \times 10^{12}$ to 3.5×10^{17} W cm^{-2}, for a fixed laser fluence in order to compare the X-ray yield. The analysis of the spectra shows that the plasma produced by the femtosecond laser at a higher intensity (3.5×10^{17} W cm^{-2}) contains feeble line radiation from He-like Mg XI ions riding on an intense continuum, without any emission from the H-like Mg XII ions. We observed that the X-ray yield (normalized with respect to the incident laser energy) of resonance line emissions from H- and He-like magnesium ions for 45 fs duration laser pulses is several orders of magnitude smaller in comparison to that for 25 ps and 3 ns duration laser pulses, even though the peak laser intensity in the 45 fs pulse irradiation was higher by five orders of magnitude. A simple analytical calculation of the ionization equilibrium time for the heated plasma, as well as that during its expansion, using a simple hydrodynamic model, shows that the time required to produce H-like ionization state is much longer than the temporal duration of the hot plasma produced with picosecond and femtosecond laser pulses, which explains the observed behaviour of the line emission.

2. Description of the experiment

The experiment was carried out using three different laser systems delivering laser pulses of duration varying from femtoseconds to nanoseconds. Pulses of 45 fs (FWHM) duration were obtained from a 10 Hz Ti:sapphire laser operated at 800 nm. The incident angle of the laser beam was set to be 45° (with respect to the laser direction). In the current experiments, laser was focussed onto a maximum intensity of $\sim 3.5 \times 10^{17}$ W cm^{-2} for a measured focal spot diameter of 30 μm. The temporal width of the laser pulse

was measured using a second-order autocorrelator. The picosecond intensity contrast ratio measured with a third-order autocorrelator was better than 10^4, and the nanosecond intensity contrast ratio, measured with a fast photodiode, was better than 10^5.

For picosecond laser irradiance, a 100 GW Nd:glass laser system ($\lambda = 1054$ nm) was used. It provided single laser pulses of 25 ps (FWHM) duration. The laser was checked for any pre-pulse (due to any leakage transmission of the rejected pulses of the mode-locked train from the pulse selector) and amplified spontaneous emission (ASE) from the amplifiers. The intensity contrast ratio was measured to be $\sim 10^5$. In the present experiment the focussed laser intensity was estimated to be $\sim 6.2 \times 10^{14}$ W cm^{-2} for a focal spot of 70 μm. An indigenously developed S-1 streak camera [26] with 5 ps resolution was used for measuring the laser pulse duration.

The nanosecond laser pulses were obtained from a 3 GW, 3 ns Nd:glass laser system operated at second harmonic ($\lambda = 527$ nm) wavelength. For this experiment, the laser pulses were focussed on planar targets to an intensity of $\sim 5 \times 10^{12}$ W cm^{-2}, for a focal spot size (diameter) of ~ 130 μm. The duration of these laser pulses was measured using a biplanar photodiode (Hamamatsu) and a fast oscilloscope (Lecroy, 500 MHz).

The X-ray line emission from the plasma produced by femtosecond, picosecond and nanosecond duration laser pulses was measured at a fixed laser fluence of $\sim 1.5 \times 10^4$ J cm^{-2}. High-resolution X-ray spectrum was recorded with an X-ray crystal spectrograph [27]. It was set to cover a wavelength ranging from 6.9 Å to 9.6 Å, with a linear dispersion of 0.26 Å/mm. This spectrograph had a planar slab of thallium acid phthalate (TAP) crystal having a double interplanar spacing ($2d$) of 25.75 Å [(0 0 1) plane]. The size of the crystal was 50 mm $\times$ 10 mm, with a thickness of 2 mm. The spectrum was recorded on a Kodak DEF-5 X-ray film (size 30 $\times$ 30 mm) placed normal to the X-rays reflected from the crystal. Two aluminized polycarbonate foils [28] (trade name B-10, energy cut-off of 0.9 keV) were used to prevent any scattered light in the plasma chamber from coupling to the film. An opaque screen was placed to prevent any X-ray emission from the plasma falling directly on the film. While using this spectrograph with femtosecond laser, it was set to record the X-ray emission with a spectral resolution of 0.013 Å in the spectral range of 7.6 Å–9.7 Å.

The film was developed using the standard procedure with D-19 developer and its optical density vs. wavelength record was obtained using a microdensitometer (Carl Zeiss) having a slit width of 80 μm, connected to a computer to record the data in digital form for further processing. The intensities of the various lines were calculated using a value of $\gamma = 0.8$ measured *in situ* by the standard step filter technique. The wavelength calibration on the film was obtained from known emission lines of H- and He-like ions of magnesium. The spectra were corrected for the transmission of the X-ray filter used with the spectrograph.

3. Results and discussion

Figure 1 shows the X-ray emission spectrum of magnesium plasma produced by 2 J, 3 ns laser pulses at an intensity of $\sim 5 \times 10^{12}$ W cm^{-2}. The spectrum was recorded in two laser shots of similar energy. Various prominent lines in the spectral range of 6.9 Å–9.6 Å are identified as transitions in He-like (Mg XI) and H-like (Mg XII) magnesium ions, viz.

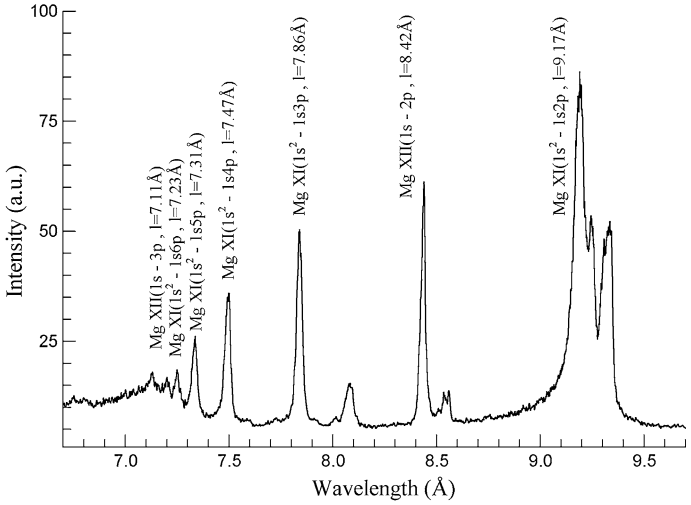

Figure 1. X-ray spectrum of magnesium plasma produced using nanosecond laser pulses at an intensity of 5×10^{12} W cm^{-2}.

(in increasing order of wavelength) Mg XII 1s–3p at $\lambda = 7.11$ Å (H-β), Mg XI $1s^2$–1s 6p at $\lambda = 7.23$ Å (He-ε), Mg XI $1s^2$–1s 5p at $\lambda = 7.31$ Å (He-δ), Mg XI $1s^2$–1s 4p at $\lambda = 7.47$ Å (He-γ), Mg XI $1s^2$–1s 3p at $\lambda = 7.86$ Å (He-β), Mg XII 1s–2p at $\lambda = 8.42$ Å (H-α), Mg XI $1s^2$–1s 2p (He-α resonance) at $\lambda = 9.17$ Å, Mg XI $1s^2$–1s 2p (He-α intercombination) at $\lambda = 9.23$ Å. Figure 2 shows the X-ray emission spectrum of magnesium plasma produced by 0.6 J, 25 ps laser pulses

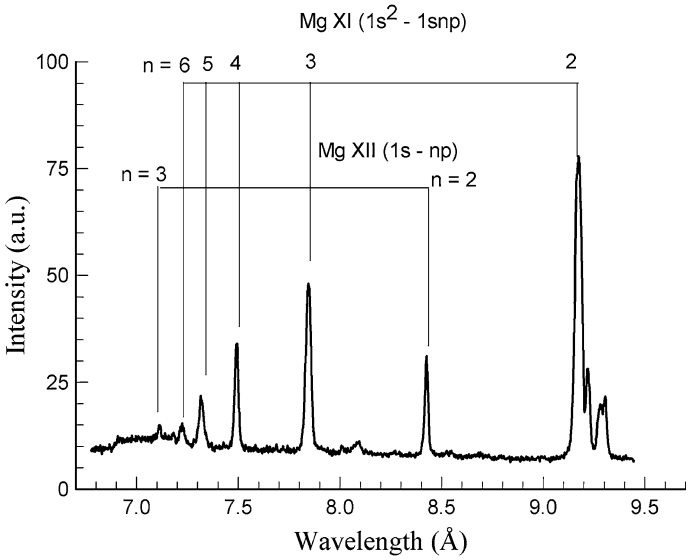

Figure 2. X-ray spectrum of magnesium plasma produced using picosecond laser pulses at an intensity of 6.2×10^{14} W cm^{-2}.

at an intensity of $\sim 6.2 \times 10^{14}$ W cm^{-2}. The spectrum was recorded in six laser shots. This spectrum is similar to the spectrum recorded with nanosecond laser pulses (shown in figure 1) except that the intensity of the line radiation from the H-like ions is significantly reduced. For instance, the intensity ratio within full profile of the magnesium He-α (resonance) to H-α line for picosecond and nanosecond plasma is $\sim$6.3 and $\sim$3.8 respectively. Figure 3 shows the X-ray spectrum of magnesium plasma produced by 110 mJ, 45 fs laser pulses at an intensity of $\sim 3.5 \times 10^{17}$ W cm^{-2}. The spectrum was recorded in 18,000 shots. Unlike in the previous two cases, the line spectrum comprising of feeble He-α at $\lambda = 9.17$ Å, He-β at $\lambda = 7.86$ Å and j, k satellites of He-α at $\lambda = 9.32$ Å is superposed over a prominent continuum. H-like emission is below the detection limit of the detector.

In order to compare the X-ray line intensities in the three cases of different pulse durations, we have derived the relative X-ray yield for different resonance lines by normalizing with respect to the incident laser energy and the number of laser shots, and to a unit distance. In figure 4, the relative X-ray yield for different line radiations, namely Mg XI $1s^2$–1s 2p (He-α), Mg XI $1s^2$–1s 3p (He-β), Mg XI $1s^2$–1s 4p (He-γ), Mg XII 1s–2p (H-α) and Mg XII 1s–3p (H-β) lines is plotted for different pulse durations used in the experiment. The error bars indicate the experimental uncertainty in measuring the intensity of the X-ray line radiation. The X-ray yield for the He-α and He-β resonance lines first increases rapidly from 45 fs to 25 ps. It is more than four orders of magnitude larger for picosecond pulse duration. An increase in X-ray yield from 25 ps up to 3 ns is only about 1.2 times for the He-β line and $\sim$1.5 times for the He-α line. For the 45 fs laser-produced plasma, the X-ray line intensity of the H-α line is below the detection limit of the detector. This gives an upper limit that X-ray yield of the H-α line radiation is smaller by a factor of 5.3×10^4 or more for the 45 fs case than for the 25 ps laser-produced

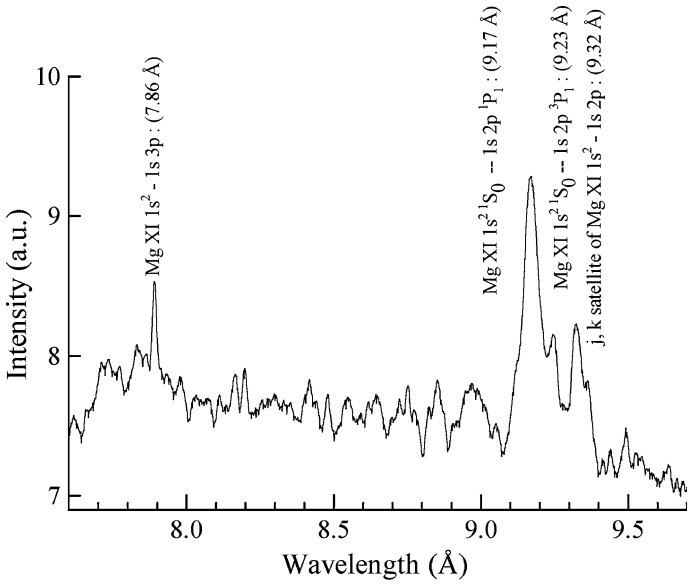

Figure 3. X-ray spectrum of magnesium plasma produced using femtosecond laser pulses at an intensity of 3.5×10^{17} W cm^{-2}.

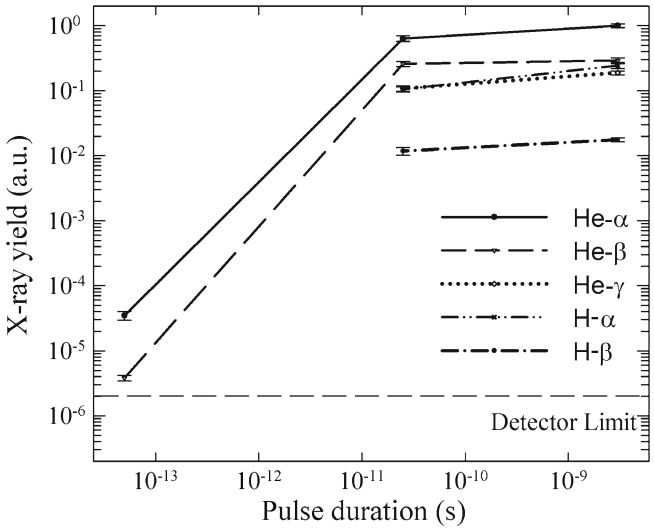

Figure 4. The relative conversion efficiency of the magnesium He-α, He-β, He-γ, H-α and H-β lines is plotted for the three different pulse durations used in the experiment. The curves are drawn to guide the eyes.

plasma. The X-ray yield of H-α, H-β and He-γ lines increases from 25 ps to 3 ns pulse duration. It becomes $\sim$2.4, $\sim$1.5 and $\sim$1.7 times for the H-α, H-β and He-γ lines respectively. Similar behaviour was also observed by Limpouch *et al* [24] in the picosecond to nanosecond pulse duration range. They also noted an increase in the conversion efficiency of the H-α and He-β resonance line radiations with the laser pulse duration. Their experimental data show that conversion efficiency of H-α and He-α increases by $\sim$50 and $\sim$7.5 times respectively while going from 1.5 ps to 1 ns pulse duration, whereas their theoretical modelling predicted an increase of three orders and two orders of magnitude for the H-α and He-α lines respectively. They assigned the difference between the observed and simulated results to the energy transport by the hot electrons.

The laser intensity can be varied either by changing the laser fluence keeping pulse duration fixed, or changing the laser pulse duration at a constant fluence. The laser intensity and the pulse duration together play an important role in governing the laser plasma interaction, especially the energy absorption and its conversion to X-ray line radiation. The intensity dependence of the X-ray line emission is mostly due to the increase in the electron temperature [22,29]. On the other hand, the laser pulse duration governs the density scale length of the plasma produced on the target, which, in combination with the laser intensity, governs the absorption of the laser energy, and the electron temperature achieved [29,30]. Moreover, the X-ray emission properties of a dense plasma in non-local thermodynamic equilibrium (NLTE), when the ionization dynamics is expected to depart more from the steady-state regime, will be different. The use of widely different laser pulses for plasma formation can be a way to investigate the ionization dynamics. However, the large difference in X-ray yield is expected to be due to the different mechanisms of interaction for the high-intensity (femtosecond) and low-intensity (nanosecond)

regimes. Nevertheless, a comparison of the relative ionization states for widely different laser pulse durations can give an estimation of the time-scale of ionization.

For the nanosecond laser pulses with a peak intensity of 5×10^{12} W cm^{-2}, the incident laser energy is absorbed in the under-dense region of the plasma, with the absorption being dominated by the inverse bremsstrahlung mechanism [31]. The plasma heating in such a situation can be well described using a self-regulating model [32]. The peak electron temperature of the corresponding region calculated on the basis of this model turns out to be 490 eV. This temperature supports the generation of both He- and H-like ion species of magnesium, as the values of the ionization potential are 1761 and 1962 eV respectively for the two species. The electron temperature of the hot plasma produced by the picosecond laser pulses may be theoretically calculated using the analytical model by Mora [32] for the laser plasma interaction relevant to the experimental conditions of short pulse–high intensity regime, with weak inverse bremsstrahlung absorption of the laser light. This gives an electron temperature of 2.4 keV. The average ionization state is expected to increase with increasing temperature. For instance, for the above estimated value of the temperature, one would expect the plasma to have a large fraction of Mg XII ions and thus an intense line emission from H-like Mg XII ions. However, as seen from figures 1 and 2, the relative intensity of the line emission from H-like Mg XII ions for picosecond plasma is $\sim$2.3 times smaller than for nanosecond plasma.

Next, for a high-intensity femtosecond laser pulse, the energy is absorbed via hot electrons generated through a number of processes, namely resonance absorption, Brunel heating, $v \times B$ heating etc. [30]. The less energetic electrons deposit their energy to heat the plasma, whereas the hot electrons penetrate into the target behind the hot plasma to generate inner-shell line radiation. At high intensity and steep density gradient, the bulk of the energy is taken by the hot electrons. The hot electron temperature for similar experimental conditions is in the range of a few tens of keV to hundreds of keV [33]. Typical fast electron relaxation time at these temperatures in short pulse laser solid interaction at solid density is of the order of few tens of ps [34], which is significantly more than the duration of fs laser pulse used in our experiment. In such a case, the X-ray emission spectra may be due to the fs laser pulse interaction with the pre-plasma produced by the pre-pulse associated with CPA-based ultrashort high-intensity laser system. The presence of density-sensitive intercombination line, whose upper level is a metastable state that is collisionally depopulated at densities higher than 10^{21} cm^{-3} [1,34], indicates that lower density pre-plasma is indeed present before the arrival of main laser pulse. The experimental observation of the lack of H-like and weak He-like ion emissions, and the presence of the Li-like satellite line, indicates that the bulk plasma is not sufficiently heated during the laser pulse. Any role of the optical field ionization in the generation of these highly charged ionic species is rather unlikely as intensity requirement for that process is $>10^{19}$ W cm^{-2} [17].

The observation of the absence of X-ray emission from the H-like ions from the femtosecond laser plasma and a relatively weak emission from the H-like ions in the picosecond laser-produced plasma indicates that the ionization dynamics departs substantially from the equilibrium regime. This can happen if the pulse duration is much shorter than the time required to reach ionization equilibrium between He- and H-like ions. In fact, the time-resolved radiation emission dynamics measurements [19,20,35] have clearly shown evidence of transient ionization regime in aluminum plasma produced

during the rising part of nanosecond pulse. Proper assessment of the ionization states would require calculations using time-dependent atomic physics. Nevertheless, ionization equilibrium time [36] can be calculated by solving the rate equations for collisional ionization, three-body recombination and radiative recombination processes, as follows:

The rate of collisional ionization is given by

$$|\partial n_e/\partial t|_S = n_e n_i S_Z, \tag{1}$$

where S_Z is the collisional ionization rate coefficient, n_e is the electron density and n_i is the ion density. The collisional ionization rate coefficient as per Bate's formula [37] for ionization from charge state Z to $Z+1$ is

$$S_Z(T_e) = 2.2 \times 10^{-6}[T_e^{1/2}\zeta_i \exp(-\chi_z^i/T_e)]/(\chi_z^i)^2 \text{ (cm}^3 \text{ s}^{-1}), \tag{2}$$

where ζ_i is the number of electrons in the ith subshell (n, l) having ionization energy χ_z^i. (χ_z^i and T_e are in eV).

Next, the rate of radiative recombination is given by

$$|\partial n_e/\partial t|_\alpha = n_e n_i \alpha_Z, \tag{3}$$

where α_Z is the radiative recombination rate coefficient for ions of charge Z. α_Z as given by Vainshtein formula [37] is

$$\alpha_Z = 8.5 \times 10^{-14}\, Z\beta^{3/2}/(\beta + 0.6) \text{ (cm}^3 \text{ s}^{-1}), \tag{4}$$

where $\beta = Z^2\chi_H$ / T_e ; χ_H is the hydrogen ionization potential.

Finally, the rate of three-body recombination is given by

$$|\partial n_e/\partial t|_{3b} = \alpha_{3b} n_e^2 n_i, \tag{5}$$

where α_{3b} is the three-body recombination rate coefficient, which as per Bate's formula [37] is

$$\alpha_{3b} = 8.75 \times 10^{-27}\, Z^3/T_e^{9/2} \text{ (cm}^6 \text{ s}^{-1}). \tag{6}$$

The ionization equilibrium time required between two adjacent ionization states may be expressed as

$$\tau_{\text{ionization}} = [1/\tau_S + 1/\tau_\alpha + 1/\tau_{3b}]^{-1}, \tag{7}$$

where

$$\tau_S = n_e/|\partial n_e/\partial t|_S\,, \tag{8}$$

$$\tau_\alpha = n_e/|\partial n_e/\partial t|_\alpha\,, \tag{9}$$

and

$$\tau_{3b} = n_e/|\partial n_e/\partial t|_{3b}\,. \tag{10}$$

The ionization equilibrium time was calculated using eqs (1)–(10). Figure 5 shows the ionization time required for the ionization of the He-like magnesium ions to H-like ions, and for the Li-like magnesium ions to He-like ions, for different values of electron temperature up to 2.5 keV, for a fixed value of electron density of 10^{21} cm^{-3} (the critical density

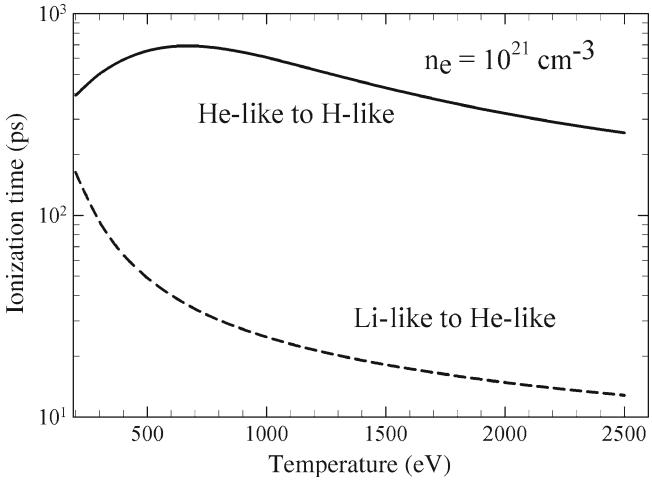

Figure 5. Ionization equilibrium time calculated for the ionization of He-like magnesium ions to H-like ions for different values of T_e (up to 2.5 keV) at a fixed value of N_e of 10^{21} cm^{-3}. The dashed curve is for the ionization of Li-like magnesium ions to He-like ions.

for 1054 nm). For instance, the ionization equilibrium time between the Li-like and the He-like ions, and between the He-like and the H-like ions at 2.4 keV electron temperature is calculated to be 15 ps and 250 ps respectively. The above values for ionization equilibrium time may vary somewhat depending on the expressions used for various processes. Nevertheless, when compared with the laser pulse duration of 25 ps, it is clear that while there is sufficient time for the production of He-like ions, this is not true for their further ionization to H-like ions. During the initial period of expansion, the temperature may remain high enough to produce high ionization states of Mg XII and Mg XI, provided the ionization equilibrium time is smaller than the plasma expansion time-scale. Further, as the plasma expands after the laser pulse is over, it undergoes evolution of density and temperature in the expanding plasma. The suppression of higher ionization stages is broadly in agreement with the theoretical results of Milchberg *et al* [10] for 100 fs laser pulses. Our results show that higher ionization stages are suppressed not only in fs laser-produced plasma, but also in the plasma produced by 25 ps laser pulses. The ionization dynamics is expected to depart more from the steady-state regime as the pulse duration is decreased to 45 fs.

A lower temperature of a few hundred eV may also be sufficient for the dominant production of H-like ions over He-like ions under the condition of ionization equilibrium. It may be looked into through the study of the temporal evolution of the emission since it is affected by both the hydrodynamics and the atomic physics effect. The same was studied by Gizzi *et al* [35] and they observed that in the case of LiF target, the emission has a characteristic time of 39 ± 4 ps, compared to the 12 ps laser pulse (FWHM) used to create the plasma. Therefore, it is important to examine the temporal evolution of the ionization time

for the electron temperature and density of the plasma undergoing hydrodynamic expansion. In principle, such a calculation would require the knowledge of temperature and density profiles, which may necessitate detailed computer or numerical simulations [11,38]. For instance, Djaoui and Rose [11] have modelled the atomic physics and hydrodynamics in ps–ns laser pulse-produced plasmas using the MEDUSA hydrodynamic code. In their model, the hydrodynamic and atomic rate equations were solved to model the non-LTE plasma relevant to X-ray laser experiments. However, one can use a simple hydrodynamic model to estimate the ionization time during plasma expansion [39]. For one-dimensional expansion of the plasma, which is valid for time $t < R/c_S$, where R is the focal spot radius and c_S is the plasma expansion speed, the electron density would scale as t^{-1}. During the adiabatic expansion after the laser pulse is over, the electron temperature T_e and the density n_e are related as $T_e \propto n_e^{\gamma-1}$. Taking $\gamma = 3$ (for one-dimensional expansion), T_e would scale with distance from the target as d^{-2} and hence $\propto t^{-2}$. The ionization equilibrium time was calculated for the plasma undergoing expansion using the density and temperature values as per the above scaling laws. It is observed that the ionization time required at any stage during expansion of the plasma far exceeds the temporal duration for which the plasma remains sufficiently hot to be able to produce the H-like ions. This further corroborates the observed poor generation of the H-like ions and relatively small intensity of the Mg XII 1s–2p line in the spectrum recorded with picosecond laser pulses, and lack of lines from H-like ions as well as negligible intensity of the lines from He-like ions in the spectrum recorded with femtosecond laser pulses.

4. Conclusions

In conclusion, a comparative spectroscopic study of the X-ray emission from the magnesium plasma produced by the femtosecond, picosecond, and nanosecond lasers has been carried out, at a fixed laser fluence (1.5×10^4 J cm^{-2}). The spectrum recorded with shorter duration laser pulses at much higher intensity does not contain line emissions from higher ionization states. The analytical calculations, using a simple hydrodynamic model, show that the ionization time required to produce higher ionization states is much larger than the temporal duration of the hot plasma. The present results give the time-scales of the ionization processes which explain the experimentally observed features of the X-ray line spectrum. The results can be used for making the optimum choice of the laser pulse duration to produce short pulse, intense X-ray line emission, and for getting to know the degree of ionization in the plasma.

Acknowledgements

The authors would like to thank R A Joshi, R K Bhat and R A Khan for their support in operating the nanosecond, picosecond and femtosecond laser systems respectively, and S R Kumbhare in setting up the experiment.

References

[1] V A Boiko, A V Vinogradov, S A Pikuz, I Yu Skobelev and A Ya Faenov, *J. Sov. Laser Res.* **6**, 85 (1985)

[2] C Reich, P Gibbon, I Uschmann and E Forster, *Phys. Rev. Lett.* **84**, 4846 (2000)
[3] D C Eder, G Pretzler, E Fill, K Eidmann and A Saemann, *Appl. Phys. B: Lasers Opt.* **70**, 211 (2000)
[4] E Martinolli *et al*, *Phys. Rev.* **E73**, 046402 (2006)
[5] K Sokolowski-Tinten and D V Linde, *J. Phys. Condens. Matter* **16**, R1517 (2004)
[6] J A Chakera, A Ali, Y Y Tsui and R Fedosejevs, *Appl. Phys. Lett.* **93**, 261501 (2008)
[7] H R Griem, *Principles of plasma spectroscopy* (Cambridge University Press, Cambridge, 1997)
[8] V Arora, J A Chakera, P A Naik, S R Kumbhare, P D Gupta and N K Gupta, *J. Appl. Phys.* **100**, 33306 (2006)
[9] P Gallents *et al*, *J. Quant. Spectrosc. Radiat. Transfer* **65**, 243 (2000)
[10] H M Milchberg, I Lyubomirsky and C G Durfee, *Phys. Rev. Lett.* **67**, 2654 (1991)
[11] A Djaoui and S J Rose, *J. Phys.* **B25**, 2745 (1992)
[12] W Theobald *et al*, *Phys. Plasmas* **13**, 043102 (2006)
[13] T W J Dzelzaims *et al*, X-ray lasers 2008, *Springer Proceedings in Physics* (Springer, Netherlands, 2009) Vol. 130, p. 537
[14] J A King *et al*, *Appl. Phys. Lett.* **86**, 191501 (2005)
[15] M Silies, H Witte, S Linden, J Kutzner, I Uschmann, E Förster and H Zacharias, *Appl. Phys.* **A96**, 59 (2009)
[16] I H Hutchinson, *Principles of plasma diagnostics* (Cambridge University Press, Cambridge, 2002)
[17] A Zhidkov and A Sasakai, *Phys. Plasmas* **7**, 1341 (2000)
[18] D Giulietti and L A Gizzi, *Riv. Nuovo Cimento* **21**, 1 (1998)
[19] L A Gizzi, C A Cecchetti, M Galimberti, A Giulietti, D Giulietti, L Labate, S Laville and P Tomassini, *Phys. Plasmas* **10**, 4601 (2003)
[20] L Labate, C A Cecchetti, M Galimberti, A Giulietti, D Giulietti and L A Gizzi, *Phys. Plasmas* **12**, 83101 (2005)
[21] J N Broughton and R Fedosejeves, *J. Appl. Phys.* **74**, 3712 (1993)
[22] D Altenbernd *et al*, *J. Phys. B: At. Mol. Opt. Phys.* **30**, 3969 (1997)
[23] F N Beg, S D Moustaizis, M Tatarakis, P Lee, A Dyson and A E Dangor, *J. Phys. D: Appl. Phys.* **31**, 2777 (1998)
[24] J Limpouch *et al*, *Laser Part. Beams* **20**, 43 (2002)
[25] L M Chen *et al*, *Phys. Plasmas* **11**, 4439 (2004)
[26] J A Chakera, M Raghuramaiah, P A Naik, P D Gupta and V K Chevokin, *Opt. Laser Technol.* **33**, 421 (2001)
[27] V Arora, S R Kumbhare, P A Naik and P D Gupta, *Rev. Sci. Instrum.* **71**, 2644 (2000)
[28] B-10 (aluminized polycarbonate) foils were supplied by Alexander Vacuum Corporation, USA
[29] U Teubner, W Theobald and C Wulker, *J. Phys. B: At. Mol. Opt. Phys.* **29**, 4333 (1996)
[30] P Gibbon and E Forster, *Plasma Phys. Control. Fusion* **38**, 769 (1996)
[31] W L Kruer, *The physics of laser plasma interactions* (Addison-Wesley, Redwood City, CA, 1988)
[32] P Mora, *Phys. Fluids* **25**, 1051 (1982)
[33] B S Rao, P A Naik, V Arora, R A Khan and P D Gupta, *J. Appl. Phys.* **102**, 63307 (2007)
[34] H Chen *et al*, *Phys. Rev.* **E76**, 56402 (2007)
[35] L A Gizzi, A Giuilietti, O Willi and D Riley, *Phys. Rev.* **E62**, 2721 (2000)
[36] C De Michelis and M Mattioli, *Nucl. Fus.* **21**, 677 (1981)
[37] G P Gupta and B K Sinha, *Phys. Rev.* **E56**, 2104 (1997)
[38] R W Lee and J T Larsen, *J. Quant. Spectrosc. Radiat. Transfer* **56**, 535 (1996)
[39] V Arora, J A Chakera, S R Kumbhare, P A Naik, N K Gupta and P D Gupta, *Laser Part. Beams* **19**, 253 (2001)